

Small world effects in evolution

Franco Bagnoli⁽¹⁾

Dipartimento di Matematica Applicata, Università di Firenze

Via S. Marta, 3 I-50139 Firenze, Italy

bagnoli@dma.unifi.it

and

Michele Bezzi⁽¹⁾

SISSA - Programme in Neuroscience

Via Beirut 2-4 I-34103, Trieste, Italy

bezzi@sissa.it

(1) also INFM sez. di Firenze, Largo E. Fermi, 2 I-50125 Firenze, Italy

February 5, 2020

Abstract

For asexual organisms point mutations correspond to local displacements in the genotypic space, while other genotypic rearrangements represent long-range jumps. We show that a small-world effect is present in evolution: even a small fraction of quenched long-range jumps makes the results indistinguishable from those obtained by assuming all mutations equiprobable. We apply this result to the evolution of a population on a smooth fitness landscape, showing that the equilibrium distribution is a Boltzmann one, in which the fitness plays the role of an energy, and mutations that of a temperature.

1 Introduction

The fundamental ingredients of evolution are mutations and selection. In order to be specific, let us assume that the genome of an individual is represented by a Boolean string of length L . In this way, the genotypic space is a Boolean hypercube with 2^L nodes. Mutations can occur both along the life of an organism or during the reproduction process. Those can be divided in point mutations, which correspond to local displacements on the genotypic hypercube, and other types of mutations or rearrangements, which imply large jumps. Mutations are quite rare, so we can safely assume that for each generation at most only one mutation occurs. For non-recombinant (asexual) organisms, the combined effects of reproduction and mutations correspond to a random walk on the genetic space. Even sexual (recombinant) populations do transmit asexually some part of their genotype, such as mitochondrial or y-chromosome DNA, to which the following analysis apply.

Organisms are also subjected to selection, which we schematise as a reduction of their survival probability. We further assume a constant environment. Selection results from several constraints and can affect the frequency of certain genotypes, or even eliminate them from the population. We classify the components of selection into static and dynamic ones. In the first class we put the constraints on the individual genome that are independent on the population distribution, such as the functionality of a

certain protein or the tuning of a metabolic path. The static part of the selection is equivalent to the concept of “fitness landscape” [1, 2]. The dynamic part of the selection originates from the competition among individuals. We assume in this schematization that the competition arises only because the population shares some external resource which is evenly distributed, i.e. we disregard the effects of the interindividual competition [3, 4]. In this limit the effects of competition do not depend on the distribution of genotypes, and simply limit the total size of the population.

The effects of the selection can be roughly schematized by assuming that certain genotypes are forbidden, so that they are eliminated from the accessible space. We thus assume for the moment that evolution takes place in a flat fitness landscape. In this frame, there are no interactions among individuals: the evolution is given by the simple superposition of all possible lineages. The probability distribution of the population in the genotypic space at a given time can be obtained by summing over all possible individual “histories” in a way similar to the path integral formulation of statistical mechanics [5]. In this view, the phylogenetic lineage of an individual is given by the path connecting the genotypes of ancestors. A point mutation corresponds to a short-range displacement in the genotypic space, while all other mutations correspond to long-range jumps.

This assumption has to fail somewhere, since otherwise evolution would be equivalent to a diffusion process, without anything favoring the formation of species. It often assumed that speciation events are rare and occur in a very short time [6], either due to some change in the fitness landscape (due to an external catastrophes like the fall of a large meteorite, or to an internal rearrangement induced by coevolution) or because small isolated populations, escaping from competition, are free to explore their genotypic space (genetic drift) and find a path to an higher fitness peak [7]. Therefore, it is usually assumed that one can reconstruct the diverging time of two species from their genotypic distance from a single speciation event [8]. It is however known from recent investigations about the small-world phenomenon [9], that diffusion is seriously affected even by a small fraction of long-range jumps [10].

The main motivations of our investigation are the following. If the short-range mutations are dominant, the evolution is equivalent to a diffusion process in the genotypic space. Assuming that the fitness landscape is formed by mountains separated by valleys, and that the crests of mountains are almost flat, then the large-scale evolution is dominated by the times needed to cross a valley by chance, while the short-scale is dominated by the neutral exploration of crests [6, 11]. Vice versa, if the long-range mutations are important (eventually via a small-world mechanism), the time to connect two genotypes does not depend on their distance nor by the shape of the fitness landscape and the fitness maxima are quickly populated. Our understanding of how evolution works could be strongly affected by the consequences of small-world effects. For instance, the speciation phenomenon should not be ascribed to a “discovery” of a preexisting niche, but rather to the formation of that niche in a given ecosystem due to internal interactions (coevolution) or external physical changes (catastrophes), after which its population is an almost immediate consequence of the small-world phenomenon.

In Section 2 we formalize our model and the mathematical representation of mutation mechanisms. Then, in Section 3, we consider the consequences of short and long-range mutations for a flat fitness landscape. In the long-range case all genomes are connected, regardless of their mutual distance: this case can be considered the equivalent of a mean-field approximation. We derive analitically the rate of spreading v and the characteristic spreading time τ of a genetically homogeneous inoculum in the short-range (v_s , τ_s) and long-range (v_ℓ , τ_ℓ) cases. In the first case, v_s is independent of the genome length L , and τ_s grows linearly with L ; the opposite happens in the long-range case. Clearly, this different behavior has dramatic evolutionary consequences as L becomes large.

In general, however, only a small set of all possible long-range mutations is observed in real organisms. We thus compute numerically the rate of spreading v in a mixed short-range and sparse long-range case: we observe a small-world effect: in the limit of large genome lengths, a vanishing fraction of long-range mutations cooperates with the short-range ones to give essentially the mean-field results.

In Section 4, we show that the effects of mutations and selection can be separated in the limit of a very smooth fitness landscape and mean-field long-range mutations. In this approximation we obtain analit-

ically that the asymptotic probability distribution is a Boltzmann equilibrium one, in which the fitness plays the role of an energy and mutations correspond to temperature. We compute numerically the asymptotic probability distribution for several fitness landscapes, finding that the equilibrium hypothesis is verified. As a nontrivial example of small-world effects in evolution, we checked numerically that this scenario still holds for a sparse long-range mutation matrix. Conclusions and perspectives are drawn in the last section.

2 The model

The genotype of an individual is represented by a string $x = (x|_1, x|_2, \dots, x|_L)$ of L Boolean symbols $x|_i = 0, 1$. Each position corresponds to a locus whose gene has two allelic forms. In this way we are modeling haploid (only one copy of each gene) organisms, i.e. bacteria or viruses or, more appropriately, more archaic, pre-biotic entities. The genome can be also viewed as a spin configuration. In this case we use the symbol $\sigma|_i = 2x|_i - 1$.

We consider two kinds of mutations: point mutations, that interchange a 0 with a 1, and all other mutations that do not alter the length of the genome (transposition and inversions). We define the distance $d(x, y)$ between two genomes x and y as the minimal number of point mutations needed to pass from x into y (Hamming distance)

$$d(x, y) = \sum_{i=1}^L (x|_i - y|_i)^2.$$

All possible genomes of length L are distributed on the 2^L vertices of an hypercube. A point mutation corresponds to a unit displacement on that hypercube (short-range jump).

The occurrence of point mutations in real organisms depends on the identity of the symbol and on its position on the genome; in the present approximation, however, we assume that all point mutations are equally likely. Moreover, since the probability of observing a mutation is quite small, we impose that at most one mutation is possible in one generation. The probability to observe a point mutation from genotype y to genotype x is given by the short-range mutation matrix $\mathbf{M}_s(x, y)$. By denoting with μ_s the probability of a point mutation per generation, we have

$$\mathbf{M}_s(x, y) = \begin{cases} 1 - \mu_s & \text{if } x = y, \\ \frac{\mu_s}{L} & \text{if } d(x, y) = 1, \\ 0 & \text{otherwise.} \end{cases} \quad (1)$$

Other types of mutations correspond to long-range jumps in the genotypic space. The simplest approximation consists in assuming all mutations equiprobable. Let us denote with μ_ℓ the probability per generation of this kind of mutations. The long-range mutation matrix, \mathbf{M}_ℓ , is defined as

$$\mathbf{M}_\ell(x, y) = \begin{cases} 1 - \mu_\ell & \text{if } x = y, \\ \frac{\mu_\ell}{2^L - 1} & \text{otherwise.} \end{cases} \quad (2)$$

In the real world, only a certain kind of mutations are possible, and in this case \mathbf{M}_ℓ is replaced by a sparse matrix $\hat{\mathbf{M}}_\ell$. We introduce a sparseness index s which is the average number of nonzero off-diagonal elements of $\hat{\mathbf{M}}_\ell$. The sum of these off-diagonal elements still gives μ_ℓ . In this case $\hat{\mathbf{M}}_\ell$ is a quenched sparse matrix, and \mathbf{M}_ℓ can be considered the average of the annealed version.

After considering both types of mutations, the overall mutation matrix is $\mathbf{M} \equiv \mathbf{M}_\ell \mathbf{M}_s$ or $\mathbf{M} \equiv \hat{\mathbf{M}}_\ell \mathbf{M}_s$ for the quenched version.

We model our population at the level of the probability distribution of genomes $\mathbf{p} \equiv \mathbf{p}(t)$, thus disregarding spatial effects. The evolution equation for \mathbf{p} is

$$p'(x) = \frac{A(x) \sum_y M(x, y)p(y)}{\bar{A}}, \quad (3)$$

where the selection function $A(x)$ corresponds to the average reproduction rate of individuals with genotype x , and $\bar{A} = \sum_x A(x)p(x)$ is the average reproduction rate of the population [1, 2, 13, 14]. We write $A(x)$ in an exponential form $A(x) = \exp(V(x))$, and we denote $V(x)$ with the term *fitness landscape*.

The selection does not act directly on the genome, but rather on the *phenotype* (how an individual appears to others). The phenotype of a given genotype can be interpreted as an array of morphological characteristics. We consider the simplest case, in which the phenotype is univocally determined by the genotype x , which is not the general case, since polymorphism or age dependence are usually present. The general mapping between genotype and phenotype is largely unknown and is expected to be quite complex. The effects of some genes are additive (non-epistatic), while others can interact in a simple (control genes) or complex (morphologic genes) way.

A possible way of approximating these effects is to use the following form for the fitness $V(x)$:

$$V(x) = \frac{\mathcal{H}}{L} \sum_{i=1}^L \sigma|_i + \frac{\mathcal{J}}{L-1} \sum_{i=1}^{L-1} \sigma|_i \sigma|_{i+1} + \mathcal{K} \eta(x), \quad (4)$$

where $\eta(x)$ is a random function of x , uniformly distributed between -1 and 1 ($\langle \eta(x)\eta(y) \rangle = \delta_{x,y}$). The “field” term \mathcal{H} represents a non-epistatic contribution to the fitness, in which all genes have equal weight. The “ferromagnetic” term \mathcal{J} represents simple interactions between pairs of genes (even though in general those are not symmetric) and corresponds to a weakly rough landscape. Finally, \mathcal{K} modulates a widely rough landscape and can be thought as an approximation of the effects of complex (spin-glass like) interactions among genes.

3 Spreading and small-world effect in a flat fitness landscape

In this section we study the case of a flat fitness landscape (no selection), i.e. $\mathcal{H} = \mathcal{J} = \mathcal{K} = 0$. In this way we are modeling the evolution on the crest of a fitness mountain, assuming that all deleterious mutations are immediately lethal (the part of genotype that can originate this kind of mutations is not considered), and that we can neglect the small variation of fitness along the crest. This landscape is the one usually considered in the theory of neutral evolution [11]. Let us assume that this crest is colonized by a founder deme genotypically homogeneous (a delta peak in the genotypic distribution). We want to obtain the average time needed to populate the crest according with the different mutation schemes. Since the fitness landscape is flat, \bar{A} is a constant. In the following we obtain the spectral properties of the mutational matrices.

Both \mathbf{M}_s and \mathbf{M}_ℓ are Markov matrices. Moreover, they are circular matrices, since the value of a given element does not depend on its absolute position but only on the distance from the diagonal. This means that their spectrum is real, and that the largest eigenvalue is $\lambda_0 = 1$. Since the matrices are irreducible, the corresponding eigenvector ξ_0 is non-degenerate, and corresponds to the flat distribution $\xi_0(x) = 1/2^L$. In analogy with circular matrices in the usual space, one can obtain their complete spectrum using the analogous of Fourier transform in a Boolean hyper-cubic space. Let us define the “Boolean scalar product” \odot :

$$x \odot y = \bigoplus_{i=1}^L x|_i y|_i,$$

where the symbol \oplus represent the sum modulus two (XOR) and the multiplication can be substituted by an AND (which has the same effect on Boolean quantities). This scalar product is obviously distributive with respect to the XOR:

$$(x \oplus y) \odot z = (x \odot z) \oplus (y \odot z).$$

Note that the operation $x \oplus y$ is performed bitwise between the two genotypes x and y .

Given a function $f(x)$ of a Boolean quantity $x \in \{0, 1\}^L$, its “Boolean Fourier transform” is $\tilde{f}(k)$ ($k \in \{0, 1\}^L$)

$$\tilde{f}(k) = \frac{1}{2^L} \sum_x (-1)^{x \odot k} f(x).$$

The anti-transformation operation is determined by the definition of the Kronecker delta

$$\delta_{k,0} = \frac{1}{2^L} \sum_x (-1)^{x \odot k},$$

and is given by

$$f(x) = \sum_k (-1)^{x \odot k} \tilde{f}(k).$$

One can easily verify that the Fourier vectors $\xi_k(x) = (-1)^{x \odot k}$ are eigenvectors of both \mathbf{M}_ℓ and \mathbf{M}_s , with eigenvalues

$$\begin{aligned} \lambda_0 &= 1, \\ \lambda_k &= 1 - \mu_\ell - \frac{\mu_\ell}{2^L - 1}, \end{aligned} \tag{5}$$

for the long-range case, and

$$\begin{aligned} \lambda_0 &= 1, \\ \lambda_k &= 1 - \frac{2\mu_s d(k, 0)}{L}, \end{aligned} \tag{6}$$

for the short-range case, where $d(x, y)$ is the Hamming distance between genotypes x and y .

We are interested in the behavior of $\rho(t)$, which is the average distance of the population from a given starting genotype, i.e.

$$\rho(t) = \sum_x p(x, t) d(x, x_0). \tag{7}$$

Assuming $x_0 = 0$. We introduce the spreading velocity v as

$$v = \left. \frac{\partial \rho}{\partial t} \right|_{t=0}.$$

The computation of $\rho(t)$ is easily performed in Fourier space, using the analogous of Parsifal theorem:

$$\begin{aligned} \sum_x f(x) g(x) &= \sum_x \sum_k \sum_{k'} \tilde{f}(k) \tilde{g}(k') (-1)^{x \odot (k \oplus k')} \\ &= 2^L \sum_k \sum_{k'} \tilde{f}(k) \tilde{g}(k') \delta_{k, k'} \\ &= 2^L \sum_k \tilde{f}(k) \tilde{g}(k), \end{aligned}$$

where we have used the property $k \oplus k' = 0$ if and only if $k = k'$ for each bit.

The Fourier transform of the distance $d(x, y)$ is obtained considering that $(-1)^{(x \oplus y) \odot 2^n}$ gives 1 if $x|_n = y|_n$ and -1 otherwise, thus

$$d(x, y) = \frac{1}{2} \left(L - \sum_{n=0}^{L-1} (-1)^{(x \oplus y) \odot 2^n} \right).$$

We obtain

$$\begin{aligned} \tilde{d}_{x_0}(k) &= \frac{1}{2^L} \sum_x d(x, x_0) (-1)^{x \odot k} \\ &= \frac{1}{2^L} \frac{1}{2} \sum_x \left(L - \sum_{n=0}^{L-1} (-1)^{(x \oplus x_0) \odot 2^n} \right) (-1)^{x \odot k} \\ &= \frac{L}{2} \delta_{k,0} - \frac{1}{2} \left(\sum_{n=0}^{L-1} (-1)^{x_0 \odot 2^n} \right) \left(\sum_x (-1)^{x \odot k \oplus 2^n} \right) \\ &= \frac{L}{2} \delta_{k,0} - \frac{1}{2} \sum_{n=0}^{L-1} (-1)^{x_0 \odot 2^n} \delta_{k,2^n}; \end{aligned}$$

i.e.

$$\tilde{d}_{x_0}(k) = \begin{cases} L/2 & \text{if } k = 0, \\ -1/2 & \text{if } k = 2^n \text{ and } x_0|_n = 0, \\ 1/2 & \text{if } k = 2^n \text{ and } x_0|_n = 1, \\ 0 & \text{otherwise.} \end{cases}$$

The probability distribution $\mathbf{p}(t)$ can be expanded on the eigenvector basis $\xi_k(x)$ of \mathbf{M} :

$$p(x, 0) = \sum_k a_k \xi_k(x) = \sum_k a_k (-1)^{x \odot k},$$

and

$$p(x, t) = \mathbf{M}^t p(x, 0) = \sum_k a_k \lambda_k^t \xi_k(x),$$

i.e.

$$\tilde{p}(k, t) = a_k \lambda_k^t.$$

Thus

$$\begin{aligned} \rho(t) &= \sum_k \tilde{d}_{x_0}(k) \tilde{p}(k, t) \\ &= \sum_k \tilde{d}_{x_0}(k) a_k \lambda_k^t \\ &= \frac{L}{2} \lambda_0^t + \sum_{n=0}^{L-1} \frac{1}{2} a_{2^n} \lambda_{2^n}^t. \end{aligned}$$

If at $t = 0$ the distribution is concentrated at $x = 0$ ($p(x, 0) = \delta_{x,0}$) then $a_k = 1$ for all k . In both the short and long-range cases, λ_{2^n} does not depend on n (see Eqs. (5)-(6)), and thus

$$\rho(t) = \frac{L}{2} (\lambda_0^t - \lambda_1^t).$$

For the short-range case we have

$$\begin{aligned} \rho_s(t) &= \frac{L}{2} \left(1 - \left(1 - \frac{2\mu_s}{L} \right)^t \right) \\ &= \frac{L}{2} \left(1 - \exp \left(t \ln \left(1 - \frac{2\mu_s}{L} \right) \right) \right) \\ &\simeq \frac{L}{2} \left(1 - \exp \left(-\frac{t}{\tau_s} \right) \right), \end{aligned}$$

and the characteristic spreading time is $\tau_s = L/2\mu_s$. For t small compared with τ_s ($L \rightarrow \infty$) we have

$$\rho_s(t) \simeq \mu_s t \equiv v_s t. \quad (8)$$

For long-range mutations we have

$$\begin{aligned} \rho_\ell(t) &= \frac{L}{2} \left(1 - \left(1 - \mu_\ell - \frac{\mu_\ell}{2^L - 1} \right)^t \right) \\ &\simeq \frac{L}{2} \left(1 - \exp \left(-\frac{t}{\tau_\ell} \right) \right) \end{aligned}$$

with $\tau_\ell = 1/\mu_\ell$. For $t \ll \tau_\ell$ ($\mu_\ell \rightarrow 0$) we have

$$\rho_\ell(t) \simeq \frac{L\mu_\ell}{2} t \equiv v_\ell t. \quad (9)$$

The behavior of $\rho(t)$ for short times, vanishing mutation probabilities and large genomes, Eqs. (8)-(9), is rather trivial. In these approximations one can neglect back mutations, and obtain the same results on a Cayley tree. However, the full analysis gives the exact behavior of $\rho(t)$ for all times.

In the general case one has $\mathbf{M} = \mathbf{M}_s \mathbf{M}_\ell$. Since \mathbf{M}_s and \mathbf{M}_ℓ share the same eigenvectors, $\lambda = \lambda_s \lambda_\ell$ and, in the previous approximations,

$$v = v_s + v_\ell. \quad (10)$$

We investigated the sparse case by numerical simulations, for some genome lengths L . As shown by Figure 1, as soon as the sparseness index $s > 0$, the numerical value of v is very near to the mean-field value of Eq. (10), suggesting a first-order transition at $s = 0$ [15]. However, the fluctuations $\chi^2(v)$ of the velocity diverge at $s = 0$ with an exponent $1/2$, as shown in Figure 2.

These results suggest the presence of a small-world phenomenon in evolution: the rare and sparse long-range mutations cooperate synergetically with the short-range ones to give essentially a mean-field effect. We checked that the previous results hold also for a non-flat (smooth) fitness landscape.

4 Path integral formulation of evolving populations

Let us introduce now a path integral formulation of Eq. (3), and in this framework we will study the small-world effect in presence of a static fitness landscape. In this case fitness A does not depend explicitly

on the whole distribution \mathbf{p} , and Eq. (3) can be linearized by using unnormalized variables $z(x, t)$ that satisfy

$$z(x, t+1) = \sum_y A(y)M(x, y)z(y, t), \quad (11)$$

with the correspondence

$$p(x, t) = \frac{z(x, t)}{\sum_y z(y, t)}.$$

In vectorial terms, Eq. (11) can be written as

$$\mathbf{z}(t+1) = \mathbf{M}\mathbf{A}\mathbf{z}(t), \quad (12)$$

where $\mathbf{M}_{xy} = M(x, y)$ and $\mathbf{A}_x = A(x)\delta_{xy}$.

When one takes into consideration only point mutations ($\mathbf{M} \equiv \mathbf{M}_s$), Eq. (11) can be read as the transfer matrix of a two-dimensional Ising model [16, 17, 18], for which the genotypic element σ_i^t corresponds to the spin in row t and column i , and $z(\sigma, t)$ is the restricted partition function of row t . The effective Hamiltonian (up to constant terms) of a possible genealogical story $\{x(t)\}$ or $\{\sigma(t)\}$ from time $1 \leq t \leq T$ is

$$\mathcal{V} = \sum_{t=1}^{T-1} \left(\gamma \sum_{i=1}^L \sigma_i(t) \sigma_i(t+1) + V(x(t)) \right), \quad (13)$$

where $\gamma = -\ln(\mu_s/(1 - \mu_s))$.

This peculiar two-dimensional Ising model has a long-range coupling along the row (depending on the choice of the fitness function) and a ferromagnetic coupling along the time direction (for small short range mutation probability). In order to obtain the statistical properties of the system one has to sum over all possible configurations (stories), eventually selecting the right boundary conditions at time $t = 1$. The bulk properties of Eq. (13) cannot be reduced in general to the equilibrium distribution of a one dimensional system, since the transition probabilities among rows do not obey detailed balance. Moreover, the temperature-dependent Hamiltonian (13) does not allow an easy identification between energy and selection, and temperature and mutation, what is naively expected by the biological analogy with an adaptive walk.

An Ising configuration of Eq. (13) corresponds to a possible genealogic story, i.e. as a directed polymer in the genotypic space [19], where mutations play the role of elasticity. It is natural to try to rewrite the model in terms of the sum over all possible paths in genotypic space.

4.1 Long-range mutations

Let us first consider the long-range mutation case. Eq. (12), reformulated according to Eq. (3), corresponds to

$$\mathbf{z}(t + \tau) = (\mathbf{A}\mathbf{M}_\ell)^\tau \mathbf{z}(t).$$

Since it is easier to consider the effects of \mathbf{A} and \mathbf{M}_ℓ separately, let us study in which limit they commute. The norm of the commutator on the asymptotic probability distribution \mathbf{p} is

$$\|[\mathbf{A}\mathbf{M}_\ell]\| = \sum_{ij} |[\mathbf{A}\mathbf{M}_\ell]_{ij} \mathbf{p}_j|,$$

and it is bounded by $\mu_\ell c$, where $c = \max_{ij} |A_{ii} - A_{jj}|$. In the limit $\mu_\ell c \rightarrow 0$ (i.e. a very smooth landscape), to first order in c we have

$$(\mathbf{A}\mathbf{M}_\ell)^\tau = \mathbf{A}^\tau \mathbf{M}_\ell^\tau + O(\tau^2 \mu_\ell c) \mathbf{A}^{\tau-1} \mathbf{M}_\ell^{\tau-1},$$

which is the analogous of the Trotter product formula.

When τ is order $1/\mu_\ell$, \mathbf{M}_ℓ^τ is a constant matrix with elements equal to $1/2^L$, and thus $\mathbf{M}_\ell \mathbf{p}$ is a constant probability distribution. If μ_ℓ is large enough, $(\mathbf{A}\mathbf{M}_\ell)^\tau = \mathbf{A}^\tau \mathbf{M}_\ell^\tau$.

The asymptotic probability distribution \tilde{p} is thus proportional to the diagonal of \mathbf{A}^{1/μ_ℓ} :

$$\tilde{p}(x) = C \exp\left(\frac{V(u(x))}{\mu_\ell}\right) \quad (14)$$

i.e. a Boltzmann distribution with Hamiltonian $V(u(x))$ and temperature μ_ℓ . This corresponds to the naive analogy between evolution and equilibrium statistical mechanics. In other words, the genotypic distribution is equally populated if the phenotype is the same, regardless of the genetic distance since we used long-range mutations.

In terms of the sum over paths [20, 5] Eq. (11) becomes

$$z(\sigma, T) = \sum_{\sigma'(T-1)} \cdots \sum_{\sigma'(0)} \exp\left(\sum_{t=0}^{T-1} -\gamma d_L(\sigma'(t+1), \sigma'(t)) - V(\sigma'(t))\right) z(\sigma'_0, 0)$$

where $\sigma'_0 = \sigma'(0)$ and $\sigma = \sigma'(T)$. In terms of directed polymers $\gamma d_L(\sigma'(t+1), \sigma'(t))$ is the bending contribution to the energy, while in term of path sums $\gamma d_L(\sigma'(t+1), \sigma'(t))$ is the kinetic energy (and γ is the mass of the particle). The relevant paths in the mean field spirit are those that insist on a given genotype for a time order $1/\mu_\ell$. Restricting the sum to the paths formed by segments of time length $1/\mu_\ell$, the kinetic energy contributes a constant term. After rescaling the time of a factor $\tau = 1/\mu_\ell$, we have a free sum of the type

$$z(\sigma, n\tau) = \sum_{[\sigma'(n)]} \exp\left(\sum_{i=0}^{n-1} \tau V(\sigma'(i))\right) z(\sigma'_0, 0)$$

which gives the Boltzmann probability distribution (14).

We have checked numerically this mapping, by iterating Eq. (3) for a time t large enough to be sure of having reached the asymptotic state. We plotted the logarithm of the probability distribution $\tilde{p}(x)$ versus the value of the Hamiltonian $V(x)$. We computed the slope $1/\mu_e$ and the average of quadratic differences χ^2 of the linear regression.

The results are shown in Figure 3. We see that the equilibrium hypothesis is well verified in the limit $\mu_\ell \gg c$; and that convergence is faster for a rough landscape.

4.2 Small-world effects

Since in reality the long-range mutations follow preferred patterns, we checked that the replacement of the long-range mutations with the combined effects of a sparse long-range and a short-range matrices do not alter these results. We tested the Boltzmann distribution Eq. (14) by computing the average of quadratic differences χ^2 of the linear regression. In Figure 4 we show that χ^2 keeps low even for very small values of the sparseness s , and that the transition point vanishes when increasing L . The slope of the line is almost constant for all values of the sparseness factor s . The mixing of long and short-range mutations has an addictive effect, at least at first order, as in the case of a flat fitness landscape. This implies that for large enough genomes the sparseness of the long range mutation matrix does not alter the statistical mechanics interpretation of selection and mutations.

4.3 Pure short-range mutations

The above results hold only qualitatively for pure short-range mutations as shown in Figure 5. A small dispersion of points in figure implies that short-range mutations are sufficiently strong to cancel out the dependence on the genotypic vicinity of strains with the same phenotype to strains with different fitness. This does not happen for the very rough landscape case, even though the linear relation is satisfied in average.

In order to obtain a quantitatively correct prediction, one has to consider that the resulting slope μ_e is related to the second largest eigenvalue λ_1 of the mutation matrix by $\mu = 1 - \lambda_1$. When the phenotype only depends on the “magnetic” term \mathcal{H} , in the asymptotic state the short-range mutations connects group of equal fitness. Thus \mathbf{A} and \mathbf{M}_s commutes and indeed, in the limit $\mu_s \rightarrow 0$, μ_e tends towards the expected values $2\mu_s/L$ of Eq. (6). In the opposite case, when the phenotype depends on the disordered term \mathcal{K} , the application of the matrix \mathbf{A} “rotates” the distribution \mathbf{p} in a way which is practically random with respect to the Fourier eigenvectors of \mathbf{M}_s . Thus, the effective second eigenvalue of the mutation matrix is given by $1 - \mu_s$, obtained averaging over all the eigenvalues of Eq (6). Consequently, we obtain $\mu_e \simeq \mu_s$, but clearly this convergence is quite slow, and is observed only in the limit $\mu_s \gg c \rightarrow 0$.

When only the \mathcal{J} term is present, one observes an intermediate case, which converges very slowly to the disordered case for $L \rightarrow \infty$.

5 Conclusions

We studied some simple models of asexual populations evolving on a smooth landscape, in the presence of point mutations (small-range jumps in genotypic space) and other genetic rearrangements (long-range jumps).

We have computed analitically the spreading velocity of an initially homogeneous inoculum on a flat fitness landscape, for the short-range and the long-range mean-field (all mutations equiprobable) cases. Since in the real situation only a small set of the all possible mutations can occur, we have also considered the quenched version of the long-range mutation matrix. In this case we have shown that a small-world effect is present, since even a small fraction of quenched long-range jumps makes the results indistinguishable from those obtained by assuming all mutations equiprobable. These results still hold for a smooth fitness landscape.

We have investigated this issue further, studying the system in the presence of a static fitness landscape using a path integral formalism. In this framework, it has been possibile to show that the equilibrium distribution is a Boltzmann one, in which the fitness plays the role of an energy, and mutations that of a temperature. We have checked numerically this result for different fitness landscapes, and a mean-field long-range mutation mechanism. As in the previous case, a small-world phenomenon appears, since similar results can be obtained using a combination of sparse long-range and short-range mutations.

We wish to acknowledge our participation to the DOCS [21] group in Florence.

References

- [1] R.A. Fisher, *The genetical theory of natural selection* (Dover, New York 1930).
- [2] S. Wright, *The Roles of Mutation, Inbreeding, Crossbreeding, and Selection in Evolution, Proc. 6th Int. Cong. Genetics, Ithaca*, **1**, 356 (1932).
- [3] F. Bagnoli and M. Bezzi, Phys. Rev. Lett. **79**, 3302 (1997), and cond-mat/9708101.
- [4] F. Bagnoli and M. Bezzi, Annual Review of Computational Physics VIII (2000)

- [5] F. Bagnoli and M. Bezzi, *Path Integral Formulation of Evolving Ecosystems*, in *Path Integrals from peV to TeV*, Edited by R. Casalbuoni et.al.(World Scientific, Singapore 1999) p. 493.
- [6] S. Gould and N. Elredge, *Paleobiology* **3**, 114 (1997); *Nature* **366**, 223 (1993).
- [7] E. Mayr, *Populations, species and evolution* (Harvard University Press, Cambridge Mass. 1970).
- [8] J. Maynard Smith, *Evolutionary genetics* (Oxford University Press, Oxford 1998).
- [9] D. J. Watts and S. H. Strogatz, *Nature* **393**, 440 (1998).
- [10] R. Monasson, *Eur. Phys. Jour. B* **12**, 60 (1999).
- [11] M. Kimura, *The neutral theory of molecular evolution* (Cambridge University Press, Cambridge 1983).
- [12] M. Doebeli, *J. Evol. Biol.* **9**, 893 (1999); U. Dieckmann and M. Doebeli, *Nature* **400**, 354 (1999).
- [13] D. L. Hartle, *A Primer of Population Genetics*, 2nd ed. (Sinauer, Sunderland, Massachusetts, 1988).
- [14] L. Peliti, *Fitness Landscapes and Evolution*, in *Physics of Biomaterials: Fluctuations, Self-Assembly and Evolution*, Edited by T. Riste and D. Sherrington (Kluwer, Dordrecht 1996) pp. 287-308, and cond-mat/9505003.
- [15] M. Argollo de Menezes, C.F. Moukarzel and T.J.P. Penna, *Europhys. Lett.* vol. 50, 5 (2000) and cond-mat/9903426.
- [16] I. Leuthäusser, *J. Stat. Phys.* **48**, 343 (1987).
- [17] P. Tarazona, *Phys. Rev. A* **45**, 6038 (1992).
- [18] T. Wiehe, E. Baake and P. Schuster, *J. Theor. Biol.* **177**, 1 (1995).
- [19] S. Galluccio, *Phys. Rev. E* **56**, 4526 (1997).
- [20] L. S. Schulman, *Techniques and Applications of Path Integration*, (John Wiley & Sons, New York 1981).
- [21] <http://www.docs.unifi.it/>

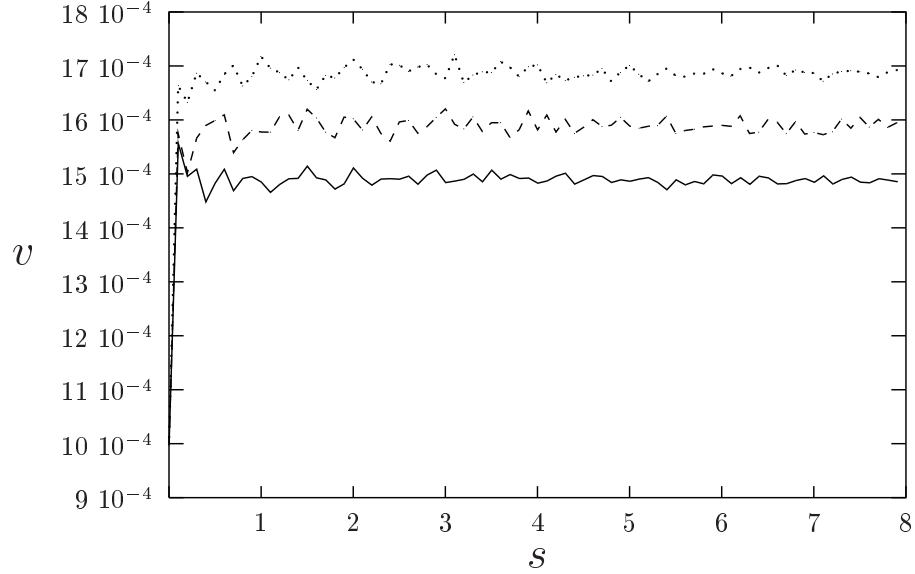


Figure 1: The spreading velocity v vs. the sparseness s for $L = 10$ (solid curve), $L = 12$ (dashed curve) and $L = 14$ (dotted curve); $\mu_\ell = 10^{-4}$ and $\mu_s = 10^{-3}$, flat fitness landscape. The mean field results $v = \mu_s + L\mu_\ell/2$ correspond to $v = 15 10^{-4}$ ($L = 10$), $v = 16 10^{-4}$ ($L = 12$), $v = 17 10^{-4}$ ($L = 14$).

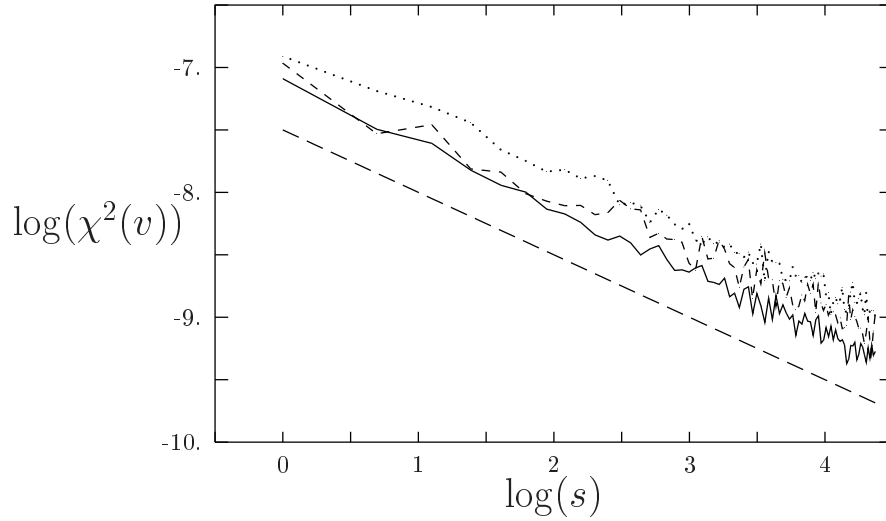


Figure 2: The fluctuations of the spreading velocity $\chi^2(v)$ vs. the sparseness s (logarithmic scale) for $L = 10$ (solid curve), $L = 12$ (dashed curve) and $L = 14$ (dotted curve); $\mu_\ell = 10^{-4}$ and $\mu_s = 10^{-3}$, flat fitness landscape. The dashed line represent the law $\chi^2(v) \sim s^{-1/2}$.

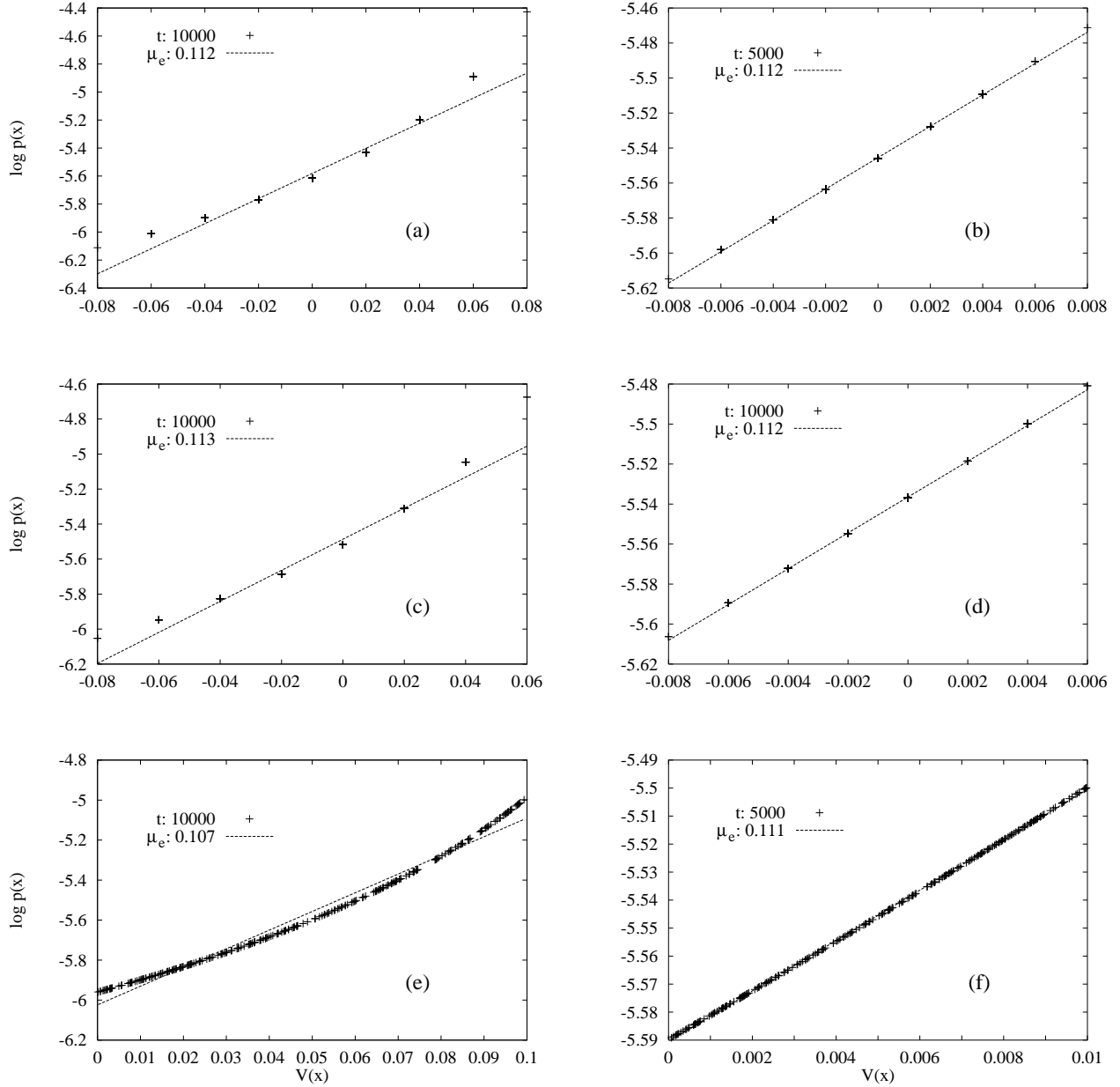


Figure 3: Numerical check for long-range mutations. In the simulations we set $L = 8$, $\mu_\ell = 0.1$ and $\mu_s = 0$. We varied \mathcal{H} (a,b), \mathcal{J} (c,d) and \mathcal{K} (e,f), setting all other parameters to zero. (a) $\mathcal{H} = 0.01$, $\mathcal{J} = 0$, $\mathcal{K} = 0$; (b) $\mathcal{H} = 0.001$, $\mathcal{J} = 0$, $\mathcal{K} = 0$; (c) $\mathcal{H} = 0$, $\mathcal{J} = 0.01$, $\mathcal{K} = 0$; (d) $\mathcal{H} = 0$, $\mathcal{J} = 0.001$, $\mathcal{K} = 0$; (e) $\mathcal{H} = 0$, $\mathcal{J} = 0$, $\mathcal{K} = 0.1$; (f) $\mathcal{H} = 0$, $\mathcal{J} = 0$, $\mathcal{K} = 0.01$. In the figures t indicates the number of generations, μ_e the reciprocal of the slope of linear regression.

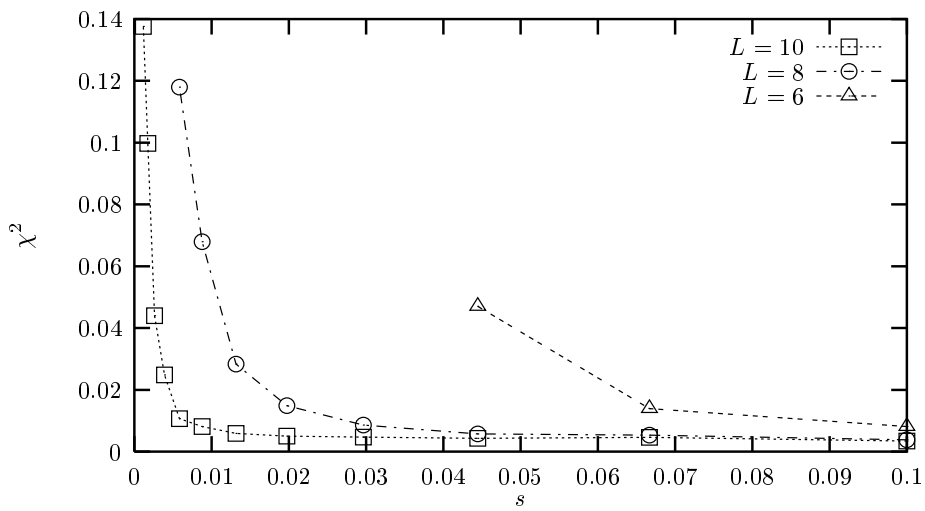


Figure 4: Scaling of χ^2 with the sparseness factor s , for three values of genome length L . $\mu_\ell = 0.1$ and $\mu_s = 0.1$, $\mathcal{H} = 0$, $\mathcal{J} = 0$, $\mathcal{K} = 0.1$

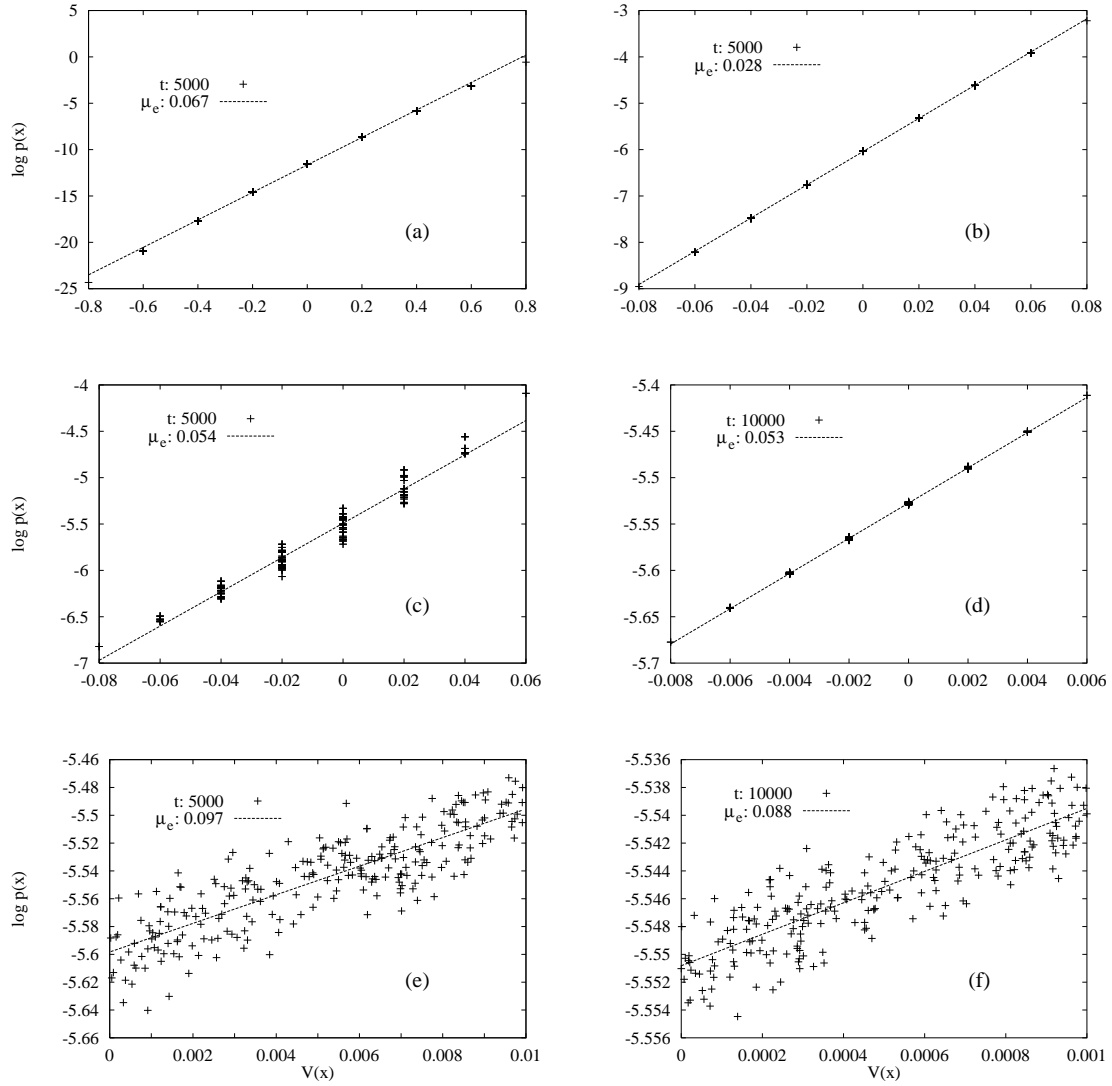


Figure 5: Numerical check for short-range mutations. In the simulations we set $L = 8$, $\mu_\ell = 0$ and $\mu_s = 0.1$. We varied \mathcal{H} (a,b), \mathcal{J} (c,d) and \mathcal{K} (e,f), setting all other parameters to zero. (a) $\mathcal{H} = 0.1$, $\mathcal{J} = 0$, $\mathcal{K} = 0$; (b) $\mathcal{H} = 0.01$, $\mathcal{J} = 0$, $\mathcal{K} = 0$; (c) $\mathcal{H} = 0$, $\mathcal{J} = 0.01$, $\mathcal{K} = 0$; (d) $\mathcal{H} = 0$, $\mathcal{J} = 0.001$, $\mathcal{K} = 0$; (e) $\mathcal{H} = 0$, $\mathcal{J} = 0$, $\mathcal{K} = 0.01$; (f) $\mathcal{H} = 0$, $\mathcal{J} = 0$, $\mathcal{K} = 0.001$. In the figures t indicates the number of generations, μ_e the reciprocal of the slope of linear regression.